

## *Chapter 8*

---

**Ebenso *et al*** investigated thiosemicarbazide derivatives AP4PT, D4PT and HP4PT as corrosion inhibitors for mild steel in sulphuric acid solution. QSAR approach was used on a composite index of some quantum chemical parameter to characterize the performance. The local reactivity has been analyzed through the Fukui and condensed softness indices in order to predict the possible sites for nucleophilic and electrophilic attacks<sup>4</sup>.

The DFT quantum chemical calculations have been performed on some pyrrolidone derivatives using Gaussian 09 and hybrid B3LYP functional density with 6-31G\* basis set<sup>5</sup>.

Quantum chemical calculations using DFT were performed on some selected triazoles, benzimidazole derivatives to determine the reactive centers which might interact with metal surface. The results showed that the adsorption would be preferentially through the benzene ring that is fused to the heterocyclic ring and through the heteroatoms. Study on protonated species of the compounds show that they have the least tendency to chemically adsorb on the metal surface<sup>6</sup>.

The inhibition efficiency of 2, 4-bisphenyl-1H-benzodiazepine (BPBD) and 2, 4-bismethoxy phenyl)-1H-benzodiazepine on corrosion of N80 steel in 15% HCl was investigated using quantum chemical studies. The mechanism was discussed in light of chemical structure and quantum chemical calculation<sup>7</sup>.

**Mondal and Taylor** compared the theoretical parameters and experiment inhibition efficiency of heterocyclic compounds – imidazole, 2-methylimidazole, benzimidazole, piperazine, histidine. High correlation between the computational mode and experimental data was obtained<sup>8</sup>.

The effect of 2,6-bis-(hydroxyl)-pyridine (P1), 2,6-bis-(chloro)-pyridine (P2) and diethyl 1,1'-(pyridine-2,6-diyl) bis (5-methyl-1H-pyrazol 2-3-carboxylate (P3) on the corrosion of steel in 1M HCl was studied by weight loss measurements, potentiodynamic and impedance spectroscopy methods by **Elmsellem *et al.*** Results of polarization studies reveal that the inhibitors act as mixed type and a very good agreement was found between gravimetric and electrochemical methods. Various thermodynamic parameters were evaluated and the inhibitor was found to obey Langmuir adsorption isotherm. Quantum chemical calculations were done based on DFT methods at B3LYP/6-31G\*\* level of theory by means of GAUSSIAN 03 set of programs. Structural parameters such

as frontier molecular orbital energies such as  $E_{\text{HOMO}}$ ,  $E_{\text{LUMO}}$ , energy gap  $\Delta E$ , absolute hardness  $\eta$ , softness  $\sigma$ , fraction of electrons transferred  $\Delta N$  and Mulliken populations have been determined. In this study the authors made an attempt in finding the structural relationship between the molecular and electronic structures and inhibition efficiency. The results of such investigation concluded a good correlation between experimental and theoretical data and it is suggested that the adsorption centre is nitrogen present in the studied compounds<sup>9</sup>.

Corrosion inhibition mechanism of two mercaptoquinoline Schiff bases-3-(phenyliminomethyl)quinoline-2-thiol, 3-((5-methylthiazol-2-ylimino)methyl) quinoline-2-thiol (MMQT) on mild steel surface was investigated by **Saha *et al.***, using quantum chemical calculations and molecular dynamics simulation. Quantum chemical parameters such as  $E_{\text{HOMO}}$ ,  $E_{\text{LUMO}}$ , energy gap ( $\Delta E$ ), dipole moment, electronegativity, global hardness have been analyzed through Fukui indices. Adsorption behavior on iron surface has been analyzed using molecular dynamic simulation<sup>10</sup>.

The inhibition effect of synthesized Schiff bases E-2-hydroxy-N' (Pyridinyl/ thio-phenylmethylene)benzohydrazide on carbon steel corrosion in 1M HCl was investigated by potentiodynamic polarization EIS, SEM and FTIR. Quantum chemical calculations were performed to evaluate molecular parameters and to correlate with the experimentally determined inhibition efficiency<sup>11</sup>.

**Obot *et al.***, investigated corrosion inhibition potential of vinylimidazole (VI) and allylimidazole (AI) for carbon steel in 1M HCl at 25 °C and were predicted theoretically using quantum chemical calculations and molecular dynamic simulations. DFT calculations indicated that VI is more reactive than AI. Theoretical conclusions were validated experimentally using polarization, impedance spectra and AFM analysis<sup>12</sup>.

The corrosion inhibition effect of red apple fruit extract for mild steel in hydrochloric acid was investigated by **Umoren *et al.***, using gravimetric and electrochemical methods at 30-60 °C. quantum chemical calculations and molecular dynamic simulations have been used to provide insights into the mechanism of major extract components with mild steel<sup>13</sup>.

**Xianghong Li *et al.***, carried out corrosion inhibition studies of mercaptopyrimidine derivatives on cold rolled steel in HCl solution. Weight loss, potentiodynamic polarization and

EIS spectroscopy have been used. Quantum chemical calculation and molecular dynamic simulations were used to analyze global and local relativities of the compounds<sup>14</sup>.

**Guo et al.**, studied the electronic parameters of benzoxazole and benzothiazole using DFT/B3LYP, MP2, and HF methods with the 6-31G (*d, p*) basis set. The quantum chemical properties such as total energy ( $T_E$ ),  $E_{HOMO}$ ,  $E_{LUMO}$ , energy gap ( $\Delta E$ ), dipole moment ( $\mu$ ), hardness ( $\eta$ ), softness ( $\sigma$ ), electronegativity index ( $\chi$ ), fraction of electrons transferred ( $\Delta N$ ), total energy change ( $\Delta E_T$ ), and electrophilicity ( $\phi$ ) were calculated. Molecular dynamics simulation studies were used to find the most stable adsorption configurations of Fe (110)/azole system in a water environment. From the investigation it was deduced from the investigation that benzothiazole have better corrosion inhibition efficiency than benzoxazole<sup>15</sup>.

Corrosion inhibition effect of benzothiazole derivatives namely, (1, 3-benzothiazol-2-amine, 6-methyl-1, 3-benzothiazol-2-amine and 2-amino-1, 3-benzothiazol-6-thiol on mild steel was studied using density functional theory (DFT) method in gas and aqueous phase by **Dehdab et al.** Quantum chemical parameters such as  $E_{HOMO}$ ,  $E_{LUMO}$ , hardness( $\eta$ ), polarisability ( $\alpha$ ) and total negative charges were calculated at the B3LYP level of theory with 6-311++G\*\* basis set. Comparison of the results in gas phase and in aqueous phase was done and it shows that trends in molecular properties are the same. Comparison of protonated species with non-protonated species reveals that protonated species are more electron deficient than the non-protonated species. Results of Atoms-in-molecule methods suggested that the interactions between the inhibitor molecules and the iron surface are partially covalent and partially electrostatic. It was concluded that all the inhibitors under study posses more than one attack center which enables multi center adsorption of the inhibitor molecules on the metal surface<sup>16</sup>.

**Yadav et al.**, experimented the corrosion inhibition efficiency of the synthesized benzothiazole derivatives namely, (Z)-5-(4-chlorobenzylidene)-3-(benzo[d]thiazol-2-yl)-2-(4-methoxyphenyl)thiazolidine-4-one, (Z)-5-(4-methoxybenzylidene)-3-(benzo[d]thiazol-2-yl)-2-(4-methoxyphenyl)thiazolidine-4-one on mild steel in HCl medium using weight loss, potentiodynamic polarization and electrochemical impedance spectroscopic techniques. The inhibition efficiency was found to increase with increase in concentration and a

maximum efficiency of about 95.8 and 97.5 % was obtained at a concentration of 150 ppm. Adsorption and activation parameters were calculated and the adsorption of the inhibitor on the surface of the mild steel was found to obey Langmuir adsorption isotherm. Studies on the effect of molecular structure on the inhibition efficiency were done using quantum chemical calculations by using Density functional theory (DFT). Evaluation of the quantum chemical parameters such as  $E_{\text{HOMO}}$ ,  $E_{\text{LUMO}}$ , energy gap, dipole moment, electronegativity, global hardness and softness were done and the results correlate well with the experimental results<sup>17</sup>.

**Udhayakala and Rajendran** studied the corrosion inhibition performance of benzothiazole derivatives namely, 1, 3-benzothiazole-2-amine (BTA) and 6-methyl-1, 3-benzothiazole-2-amine (MBTA) for mild steel in 1N HCl using density functional theory (DFT). The inhibition efficiency of the investigated compounds obtained through theoretical calculations increase with increase in HOMO and decrease in energy gap. Electronic parameters calculated suggests that MBTA shows greater inhibition efficiency than BTA due to the presence of electron donating nature of the methyl group which makes the benzene ring to react with the metal d-orbital resulting in stronger adsorption<sup>18</sup>.

**Chakib *et al.***, investigated the corrosion inhibition behavior of (E)-4-(2,3-Dihydro-1,3-benzothiazol-2-ylidene)-3-methyl-1-phenyl-1H-pyrazol-5(4H)-one on mild steel corrosion in 1M HCl by using gravimetric and electrochemical techniques. Quantum chemical calculation are done using Gaussian-09 software package. Parameters like reactive sites of the present molecule have been analyzed through Fukui indices. The results of the investigation concluded that the inhibitor molecule evenly distribute over the steel surface<sup>19</sup>.

### 8.3 Results and discussion

Theoretical quantum chemical calculations with neutral form of inhibitors have been reported to be a good approach to correlate the experimentally determined inhibition efficiency order. Figure 8.1 - 8.4 show the optimized structure, HOMO, LUMO density of the studied molecules and represent the lowest energy geometry to each molecule.

The HOMO gives information about the regions in a molecule with the most energetic electrons. These electrons are likely to be donated to the electron poor species<sup>20</sup>. It is evident from the figures that HOMO is spread throughout the benzodiazepine ring

especially on the benzene ring fused to the heterocyclic ring and on the N atoms of the diazepine ring, which implies that these are the main adsorption centers.

LUMO is unoccupied orbital that has lowest energy and gives information about the regions in a molecule that have the highest tendency to accept electrons from an electron rich species. Analysis of figures show that highest LUMO density is also located on the benzodiazepine ring which suggest that the benzene ring fused to diazepine ring is the site for receiving electrons from metal orbitals.

Figure 8.3-8.4 shows the optimized geometry, HOMO and LUMO density distribution of benzothiazepine (EPBTZ), benzoxazepine (EPBOZ) and benzodiazepine (EPBD). In EPBTZ and EPBOZ also the HOMO and LUMO densities are located on the benzoheteroazepines ring and the phenyl substituent. As is shown, the density is maximum only in benzothiazepine.

The quantum chemical parameters such as  $E_{\text{HOMO}}$ ,  $E_{\text{LUMO}}$ ,  $\Delta E$  ( $E_{\text{HOMO}}-E_{\text{LUMO}}$ ), ionization potential ( $I = -E_{\text{HOMO}}$ ) and electron affinity ( $A = -E_{\text{LUMO}}$ ) have been computed. The values of  $I$  and  $A$  were used to calculate electronegativity ( $\chi$ ) and global hardness ( $\eta$ ) for all the molecules using the relation,

$$\chi = \frac{I+A}{2} \quad \text{and} \quad \eta = \frac{I-A}{2}$$

Global softness is the reverse of hardness

$$\sigma = \frac{1}{\eta}$$

The fraction of the electrons transferred from the inhibitor molecule to the metallic atom,  $\Delta N$  was calculated as

$$\Delta N = \frac{\chi_{\text{Fe}} - \chi_{\text{Inh}}}{2(\eta_{\text{Fe}} + \eta_{\text{Inh}})}$$

Where  $\chi_{\text{Fe}} = 7\text{eV}$  and  $\eta_{\text{Fe}} = 0$  since for a metallic bulk  $I=A$ .

$E_{\text{HOMO}}$  represents the tendency of the inhibitor to donate electrons to the unoccupied d-orbitals of metals. Higher the  $E_{\text{HOMO}}$  value of the inhibitor better is the tendency to donate electrons to the acceptor molecules, in the case of corrosion process-it

is the metal atoms (Fe atoms).  $E_{LUMO}$  represents the ability of the molecule to accept electrons from the metal surface. Lower the  $E_{LUMO}$  better is the ability to accept electrons from the metal surface so as to form back bonding. The energy gap,  $\Delta E$  ( $E_{HOMO}-E_{LUMO}$ ) should be low to render good inhibition efficiency.

In the present study three benzodiazepines from series I and three from series II have been selected and the computed quantum chemical parameters are tabulated for the two series (Tables 8.1 and 8.2).

For series I, the experimental order of inhibition efficiency for the selected benzodiazepines is MDPBD > DPBD > TMBD.  $E_{HOMO}$  is higher for MDPBD than that of the other two compounds (-5.15 eV) but DPBD has lower value (-5.26 eV) than TMBD.  $E_{LUMO}$  should be low which correlates well with experimental order of IE.  $\Delta E$  also agrees very well with experimental order i.e. low for MDPBD (3.76 eV), next for DPBD (3.94 eV) and for TMBD (4.53 eV).

For series II benzodiazepines  $E_{HOMO}$  is high for TMPBD (-5.18 eV) agreeing with experimental value.  $E_{LUMO}$  values did not correlate and the order being EPBD < TMPBD. But  $\Delta E$  value is in good agreement with the experimental results. TMPBD has lowest value than EPBD and MBD has highest among the three compounds.

A lower value of ionization potential and higher value of electron affinity enhance the inhibition efficiency. Both the values agree for MDPBD (series I diazepine) and EPBD. Good correlation was observed for electron affinity of series I benzodiazepines. In series II, compounds TMPBD has lower ionization potential. But EPBD has higher electron affinity. Global hardness and softness are important properties to measure the molecular stability and reactivity based on HSAB concept. Soft molecules are more reactive than hard molecules, because they can offer electrons easily to an acceptor molecule<sup>9</sup>. In a corrosion system, the inhibitor acts as a Lewis base while the metal acts as a Lewis acid. Bulk metals are soft acids and thus soft base inhibitors are most effective for acid corrosion of metals<sup>21</sup>. Hence good corrosion inhibitors are characterized by highest value of global softness or least values of hardness. For the two series of benzodiazepines chosen, very good correlation was obtained with experimentally determined inhibition efficiency order. Softness is higher for MDPBD (series I) and TMPBD (series II). The global hardness follows the reverse trend.

The quantum chemical indices were computed for one benzothiazepine (EPBTZ) and one benzoxazepine (EPBOZ) and compared with the corresponding benzodiazepine (EPBD). The data are recorded in Table 8.3. Analysis of the data revealed a very good correlation of the quantum chemical indices and experimental inhibition efficiency order observed for benzothiazepine, benzodiazepine and benzoxazepine.  $E_{\text{HOMO}}$  is highest,  $E_{\text{LUMO}}$  is least (-1.61 eV) and  $\Delta E$ , the energy gap is smallest (3.77 eV) for EPBTZ. EPBTZ has high electron affinity compared to the other two and has highest value of global softness. For benzoxazepines, the  $E_{\text{HOMO}}$  is lower (-5.63 eV),  $E_{\text{LUMO}}$  is higher (-1.04),  $\Delta E$  is higher (4.22 eV). It shows higher ionization potential and lower electron affinity and global softness, but higher value of hardness. Hence it can be considered as a poor inhibitor compared to the corresponding benzothiazepines and benzodiazepine.

### **Fukui functions**

The reactive regions in a molecule can be analyzed using Fukui indices. These represent the regions in a molecule susceptible for electrophilic and nucleophilic attack<sup>22</sup>. Fukui functions can be evaluated using Mulliken population analysis of atoms in a molecule depending on the direction of electron transfer.

$$f_k^+ = q_k(N+1) - q_k(N) \text{ for nucleophilic attack and}$$

$$f_k = q_k(N) - q_k(N-1) \text{ for electrophilic attack}$$

where  $q_k$  is the gross charge of atom 'k' in the molecule; N corresponds to the number of electrons in the molecule; (N+1) corresponds to an anion with an electron added to the LUMO of the neutral molecule; N-1 corresponds to the cation with an electron removed from the HOMO of the neutral molecule<sup>23</sup>. The calculated charges for the neutral molecules and charged species ( $q(N)$ ,  $q(N+1)$ ,  $q(N-1)$ ) and the Fukui indices  $f_k^+$  and  $f_k$  of the various heteroatoms in the six benzodiazepines tested are given in Table 8.4 and 8.5. In the case of corrosion inhibitor  $f_k^+$  is used to indicate the site for nucleophilic attack (when the molecule is accepting electrons),  $f_k$  indicates the site for electrophilic attack i.e. when the molecule is donating electrons to the metal atoms<sup>24</sup>. In order to simplify the discussion, the Fukui functions over the hetero atoms can be considered.



Analysis of  $f_k^-$  values of series I benzodiazepines showed (Table 8.5) that  $f_k^-$  value of N12 is highest for MDPBD (0.077481) compared to the  $f_k^-$  values of N12 for DPBD or TMBD (0.05 and 0.073).  $f_k^-$  values for N11 is also higher for MDPBD.  $f_k^+$  values of N11 and N12 are also maximum for MDPBD. Inspection of the Table 8.4 shows that among the benzodiazepines of II series  $f_k^-$  is maximum on N11 of TMPBD Compared to N11 of EPBD and MBD (0.0244). On the other hand  $f_k^-$  values on N12 are higher for MBD and EPBD. Considering N11 and N12 as the sites for electron donating, TMPBD is more susceptible for adsorption and reflects its highest inhibition performance. The HOMO location on these compounds also agrees with the atoms that exhibit greatest values of Fukui indices, which indicates the sites by which the molecule would be adsorbed on the metal surface.

The Mulliken charges and the Fukui indices of the heteroatoms of benzothiazepine (EPBTZ), benzodiazepine (EPBD) and benzoxazepine (EPBOZ) are recorded in Table 8.6. Inspection of the values showed that for EPBTZ, the  $f_k^-$  value is highest for S11 (0.0942) compared to N11 of EPBD having 0.02449 and O11 of benzoxazepine EPBOZ (0.0223). This shows that the sulphur atom is the most susceptible site for electrophilic attack. The Fukui indices for N12 of the three compounds show that N12 of benzodiazepine is most susceptible for electrophilic attack. The  $f_k^+$  values on O36, O38 of EPBTZ are higher than that of O38, O40 of EPBD which indicate that the oxygen atoms in benzothiazepine are the most susceptible sites for nucleophilic attack. These values confirm the experimental order of corrosion inhibition efficiency.

### **Protonation of inhibitors**

Organic compounds containing nitrogen atoms have high tendency to undergo protonation in acidic solution. Hence it is interesting to study the influence of protonation on the molecular structure and the molecular parameters. The study was carried out for some selected benzodiazepines namely MDPBD, DPBD, TMBD and MBD. Geometry optimization was carried out for all possible structures with different sites of protonation. The results of the calculation on the different possible sites for protonation show that the preferred site for protonation is N12. This is the less sterically hindered site because there are no other protons present. Moreover this is the common position of all the selected compounds.

Figure 8.5-8.6 shows the optimized geometries of the protonated species together with the corresponding HOMO and LUMO. The quantum chemical parameters are given in Table 8.7.  $E_{\text{HOMO}}$  and  $E_{\text{LUMO}}$  of the protonated inhibitors increased. This means that the tendency to donate electrons increased and tendency to accept electrons decreased for the protonated species. But the value of  $\Delta E$  decreased for all the selected benzodiazepines. Lower ionization energy and higher electron affinity indicate better inhibition efficiency. The ionization potential decreases for all the protonated species relative to non-protonated molecules. The global softness of the protonated forms ( $\sigma$ ) are greater compared to neutral molecules. This implies that the protonated form has greater reactivity than non protonated form i.e. the protonated species have greater tendency to adsorb on metal surface than the non-protonated species.

From the optimized geometry and HOMO, LUMO pictures and from the quantum chemical parameters, it can be concluded that the benzodiazepine ring is the main adsorption centre. One of the phenyl substituent is also involved by extending conjugation. The other phenyl ring with substituent influences the electron density on the adsorption site.

## CHAPTER-8

# QUANTUM CHEMICAL STUDIES

### 8.1 Introduction

Chapter 4 and 5 dealt with experimental evaluation of corrosion inhibition performances of benzodiazepines, benzothiazepines and benzoxazepines in 1M Sulphuric acid. In chapter 6, a comparative study has been carried out for corrosion of copper, mild steel and aluminium in 1M H<sub>2</sub>SO<sub>4</sub> with four selected benzodiazepines as inhibitors. Weight loss, potentiodynamic polarization and electrochemical impedance spectroscopic techniques have been used. Surface morphological analysis (SEM, AFM) were carried out to confirm the presence of adsorbed inhibitor molecules on the metal surface.

In order to support experimental data, theoretical calculations were carried out which provide molecular level understanding of the observed experimental behavior. Quantum chemical calculation is a good tool applied in the structural and performance research of corrosion inhibitors. Density functional theory is an efficient quantum chemistry computing method, which can provide accurate information of geometrical configuration and electron distribution. It is widely applied in the analysis of corrosion inhibition performance and the interaction of corrosion inhibitors and interfaces<sup>1,2</sup>.

In the present investigation, quantum chemical calculation using DFT was employed to explain the observed experimental order of inhibition efficiencies of some selected benzodiazepines of the two series. The study was extended to one benzothiazepine (EPBTZ) and benzoxazepine (EPBOZ) and correlated with the experimental data.

Before proceeding to the results and discussions, recent literature survey, in this field is summarized.

### 8.2 Review of Literature

The inhibition effect of 3,4-dihydropyrimidin-2(1H)-ones (DHPM1) on the corrosion of mild steel in hydrochloric acid medium was investigated by **Dilipkumar Yadav *et al.*** using weight loss and electrochemical techniques. Electronic properties obtained using quantum chemical studies correlated with experimental inhibition efficiencies<sup>3</sup>.

## References

1. Popova A, Christov M, Raicheva S, *Corros. Sci.*, **46** (2004) 1333.
2. Jianfang zhu, Shuangkou Chen, *Int. J. Electrochem. Sci.*, **7** (2012) 11884.
3. Dileep Kumar Yadav, Maiti B, Quraishi M A, *Corros. Sci.*, **52** (2010) 3585.
4. Ebenso E E, Isabirye D A, Eddy N O, *Int. J. Mol. Sci.*, **11** (2010) 2473.
5. Bouklah M, Harek H, Touzani R, Hammouti B, Harek Y, *Arab. J. Chem.*, **5** (2012) 163.
6. Kabanda M M, Murulana L C, Ozcan M, Karadag F, Dehri I, Obot I B, Ebenso E E, *Int. J. Electrochem. Sci.*, **7** (2012) 5035.
7. Kumar S , Sharma D, Yadav P, Yadav M, *Ind. Eng. Chem. Res.*, **52** (2013) 14019.
8. Mondal S K, Taylor S R, *J. Electrochem. Soc.*, **161** (2014) C476.
9. Elmsellem H, Basbas N, Chetouani A, Aouniti A, Radi S, Messali M, Hammouti B, *Port. Electrochim. Acta*, **32** (2014) 77.
10. Saha S K, Ghosh P, Hens A, Murmu N C, Banerjee P, *Physica E Low Dimens Syst Nanostruct.*, **66** (2015) 332.
11. Shahabi S, Norouzi P, Ganjali M R, *Int. J. Electrochem. Sci.*, **10** (2015) 2646.
12. Obot I B, Umoren S A, Gasem Z M, Suleiman R, El-Ali B, *J. Ind. Eng. Chem.*, **21** (2015) 1328.
13. Umoren S, Obot I B, Gasem Z, Adewale N, Odewunmi N A, *J. Dispers. Sci. Tech.*, **36** (2015) 789.
14. Li X, Xie X, Deng S, Du G, *Corros.Sci.*, **92** (2015) 136.
15. Guo L, Zhang S T, Lv T M, Feng W J, *Res Chem. Intermed.*, **41** (2015) 3729.
16. Dehdab M, Shahraki M, Habibi-Khorassani S M, *Iran J Sci. Technol.*, **39A3** (2015) 311.
17. Yadav M, Sushil Kumar, Neelam Kumari, Indra Bahadur, Ebenso E E, *Int. J. Electrochem. Sci.*, **10** (2015) 602.

18. Udhayakala P, Rajendiran T V, *Der Pharma Chem.*, **7** (2015) 92.
19. Chakib I, Elmsellem, Sebbar N K, Essassi E M, Fichtali I, Zerzouf A, Ouzidan Y, Aouniti A, El Mahi B, Hammouti B, *Der Pharma Chem.*, **8** (2016) 380.
20. Kabanda M M, Murulana L C, Ozcan M, Karadag F, Dehri I, Obot I B, Ebenso E E, *Int. J. Electrochem. Sci.*, **7** (2012) 5035.
21. Fouda A S, Eldeosoky A M, Elmorsi M A, Fayed T A, Atia M F, *J. Electrochem. Sci.*, **8** (2013) 10219.
22. Obi-Egbedi N O, Obot I B, El Khaiary M I, Umoren S A, Ebenso E E, *J. Electrochem. Sci.*, **6** (2011) 5649.
23. Obi-Egbedi N O, Obot I B, *Corros. Sci.*, **53** (2011) 263.
24. Khaled K F, *Corros. Sci.*, **52** (2010) 3225.

*Tables*

---

**Table 8.1** Quantum Chemical parameters for benzodiazepines (series I)

<b>Inhibitor</b>	<b>E<sub>HOMO</sub>(eV)</b>	<b>E<sub>LUMO</sub>(eV)</b>	<b>ΔE(eV)</b>	<b>I(eV)</b>	<b>A(eV)</b>	<b>κ(eV)</b>	<b>η (V)</b>	<b>σ</b>
<b>MDPBD</b>	-5.15	-1.40	3.75	5.15	1.40	3.28	1.88	0.53
<b>DPBD</b>	-5.26	-1.31	3.95	5.26	1.31	3.28	1.97	0.50
<b>TMBD</b>	-5.16	-0.61	4.5	5.16	0.61	2.88	2.45	0.40

**Table 8.2** Quantum Chemical parameters for benzodiazepines (series II)

<b>Inhibitor</b>	<b>E<sub>HOMO</sub>(eV)</b>	<b>E<sub>LUMO</sub>(eV)</b>	<b>ΔE(eV)</b>	<b>I(eV)</b>	<b>A(eV)</b>	<b>κ(eV)</b>	<b>η eV)</b>	<b>σ</b>
<b>TMPBD</b>	-5.18	-1.28	3.89	5.18	1.28	3.23	1.95	0.512
<b>EPBD</b>	-5.34	-1.41	3.93	5.34	1.41	3.37	1.96	0.510
<b>MBD</b>	-5.28	-0.58	4.70	5.28	0.58	2.93	2.35	0.42

**Table 8.3** Quantum chemical parameters for benzothiazepine, benzoxazepine and benzodiazepine

<b>Inhibitor</b>	<b>E<sub>HOMO</sub>(eV)</b>	<b>E<sub>LUMO</sub>(eV)</b>	<b>ΔE(eV)</b>	<b>I(eV)</b>	<b>A(eV)</b>	<b>κ(eV)</b>	<b>η eV)</b>	<b>σ</b>
<b>EPBTZ</b>	-5.38	-1.61	3.77	5.38	1.61	3.49	1.88	0.53
<b>EPBOZ</b>	-5.63	-1.04	4.22	5.63	1.04	3.33	2.29	0.43
<b>EPBD</b>	-5.34	-1.41	3.93	5.34	1.41	3.37	1.96	0.51

**Table 8.4** Mulliken charges and Fukui indices for the three selected benzodiazepine derivatives (series I)

Inhibitor	Atom	$q_N$	$q_{N+1}$	$q_{N-1}$	$f^+k$	$f^-k$	$f^0k$
<b>MDPBD</b>	N11	-0.5852	-0.5269	-0.5697	0.0664	-0.0154	0.0126
	N12	-0.5372	-0.4612	-0.6146	0.0592	0.0774	0.0410
<b>DPBD</b>	N11	-0.5910	-0.5564	-0.5875	0.0345	0.0034	0.0155
	N12	-0.5710	-0.5204	-0.6369	0.0505	0.0659	0.0582
<b>TMBD</b>	N11	-0.5933	-0.5263	-0.5771	0.0664	-0.0162	0.0251
	N12	-0.5205	-0.4612	-0.5944	0.0592	0.0739	0.0666

**Table 8.5** Mulliken charges and Fukui indices of heteroatoms for the three selected series II benzodiazepine derivatives (series II)

Inhibitor	Atom	$q_N$	$q_{N+1}$	$q_{N-1}$	$f^+k$	$f^-k$	$f^0k$
<b>TMPBD</b>	N11	-0.5671	-0.5488	-0.5740	0.0188	0.0684	0.0125
	N12	-0.5759	-0.5226	-0.6861	0.05321	0.0427	0.0479
	O38	-0.5282	-0.5304	-0.5399	-0.0022	0.0117	0.0047
	O43	-0.5422	-0.5367	-0.5419	0.0054	-0.0002	0.0025
	O48	-0.5405	-0.5343	-0.5420	0.0061	0.0015	0.0038
<b>EPBD</b>	N11	-0.5989	-0.5514	-0.5744	0.0047	-0.0244	0.0114
	N12	-0.5283	-0.5272	-0.6780	0.0010	0.0894	0.0452
	O38	-0.5590	-0.5480	-0.5786	0.0110	0.0196	0.0153
	O40	-0.5414	-0.5134	-0.5524	0.0279	0.0110	0.0194
<b>MBD</b>	N11	-0.5968	-0.5350	-0.5724	0.0618	-0.0244	0.0187
	N12	-0.4827	-0.4600	-0.5784	0.0226	0.0957	0.0591
	O34	-0.5594	-0.5369	-0.5835	0.0225	0.0240	0.0232



**Table 8.6** Mulliken charges and Fukui indices for benzothiazepine, benzoxazepine and benzodiazepine

Inhibitor	Atoms	$q_N$	$q_{N+1}$	$q_{N-1}$	$f^+k$	$f^-k$	$f^0k$
<b>EPBTZ</b>	S11	0.1086	0.2861	0.0144	0.1775	0.0942	0.1358
	N12	-0.5697	-0.4551	-0.5554	-0.1145	-0.0143	0.0501
	O36	-0.5682	0.1368	0.1091	0.7050	-0.6773	0.0138
	O38	-0.5432	0.1371	0.0852	0.7114	-0.6595	0.0259
<b>EPBOZ</b>	O11	-0.5595	-0.5371	-0.5681	0.0086	0.0223	0.0154
	N12	-0.5262	-0.5081	-0.6218	0.0955	0.0180	0.0568
	O36	-0.5559	-0.5269	-0.5701	0.0141	0.0290	0.0216
<b>EPBD</b>	N11	-0.5989	-0.5514	-0.5744	0.0047	-0.0244	0.0114
	N12	-0.5283	-0.5272	-0.6780	0.0010	0.0894	0.0452
	O38	-0.5590	-0.5480	-0.5786	0.0110	0.0196	0.0153
	O40	-0.5414	-0.5134	-0.5524	0.0279	0.0110	0.0194

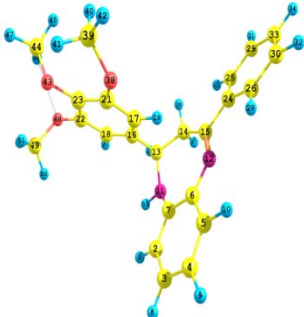
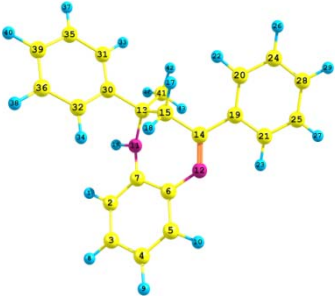
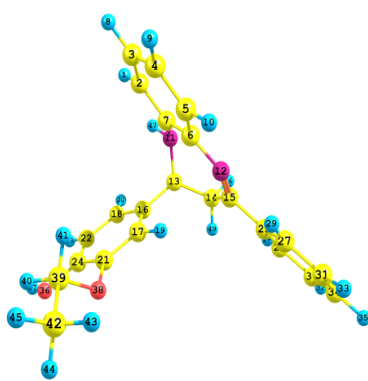
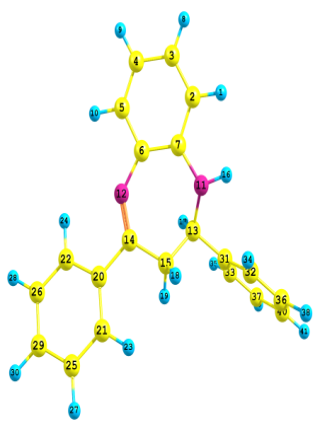
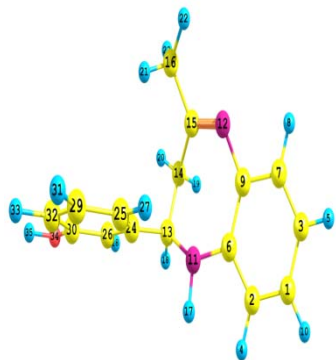
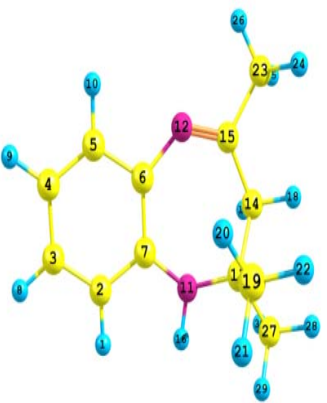
**Table 8.7** Quantum Chemical parameters for protonated benzodiazepines

Inhibitor	$E_{HOMO}(eV)$	$E_{LUMO}(eV)$	$\Delta E(eV)$	$I(eV)$	$A(eV)$	$\alpha(eV)$	$\eta(eV)$	$\sigma$
<b>MDPBD</b>	-3.35	-0.70	2.64	3.35	0.70	2.02	1.35	0.74
<b>DPBD</b>	-3.29	-2.26	1.03	3.29	2.26	2.77	0.51	1.96
<b>TMBD</b>	-3.42	-0.25	3.16	3.42	0.25	3.29	1.58	0.63
<b>MBD</b>	-3.01	-0.36	2.65	3.01	0.36	1.68	1.32	0.75

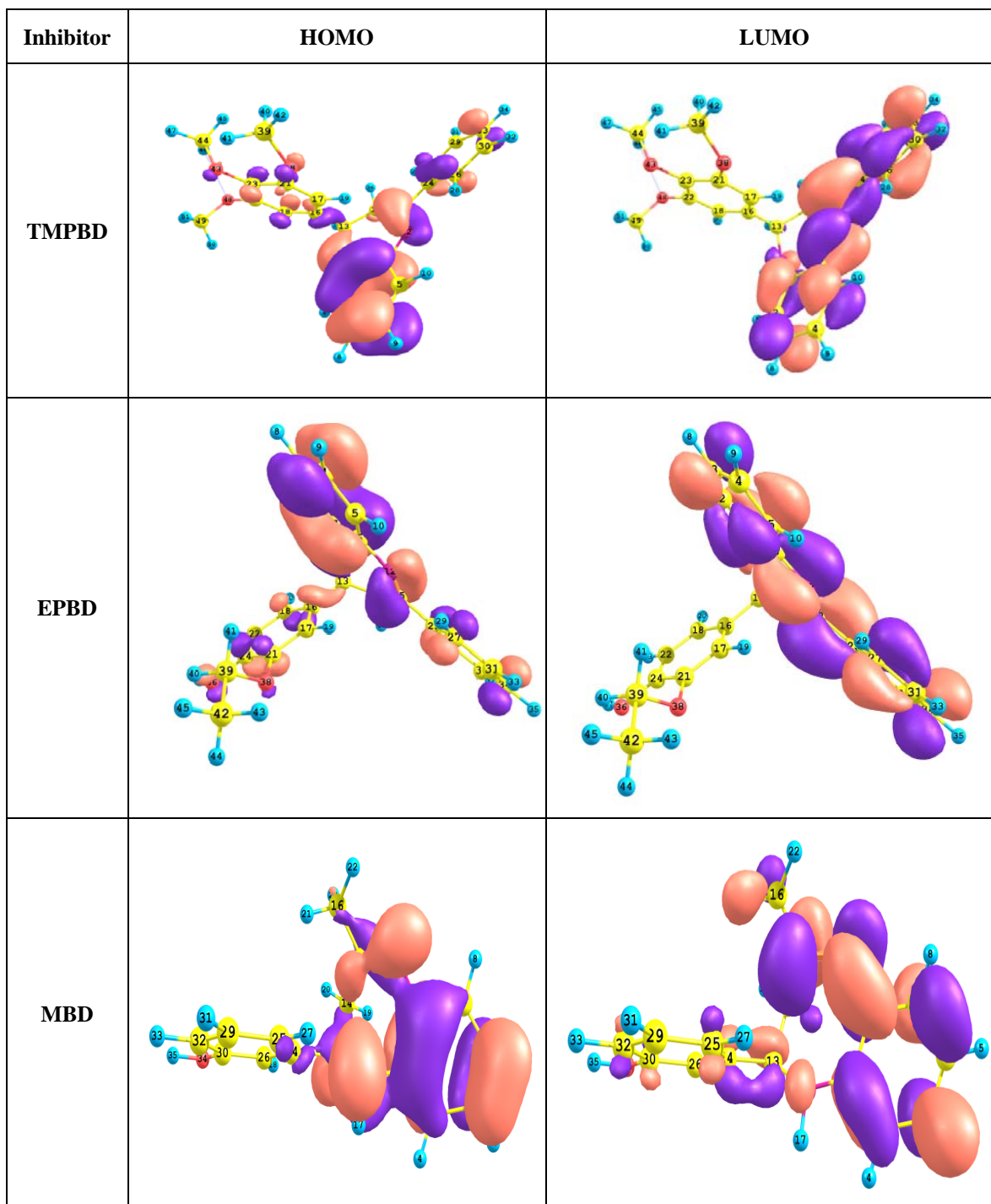
*Figures*

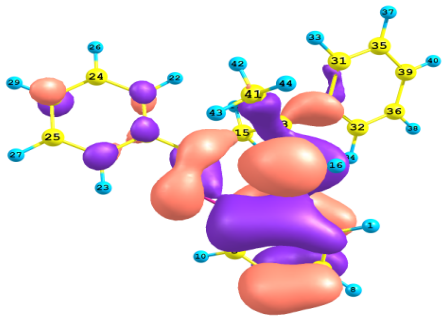
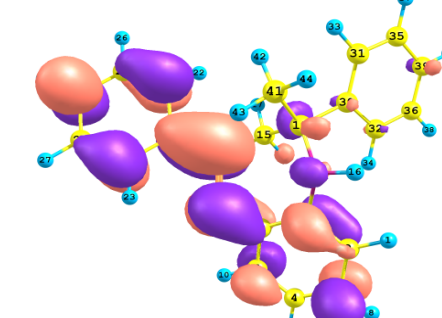
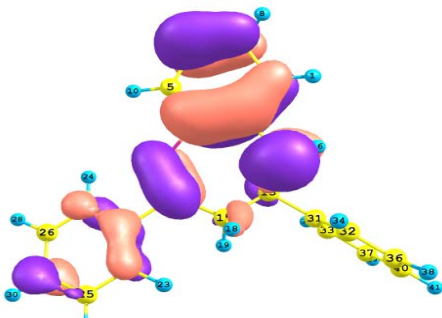
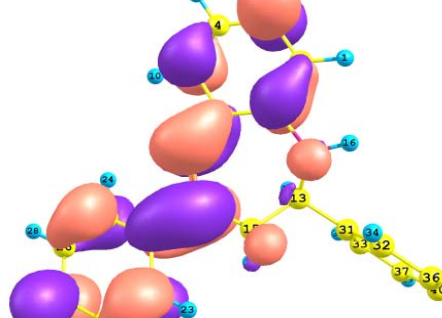
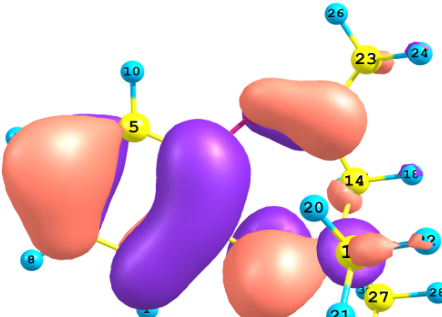
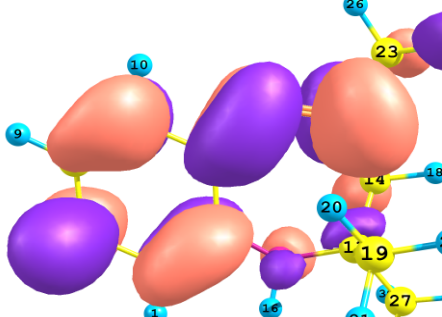
---

**Figure 8.1** Optimized geometry of benzodiazepines

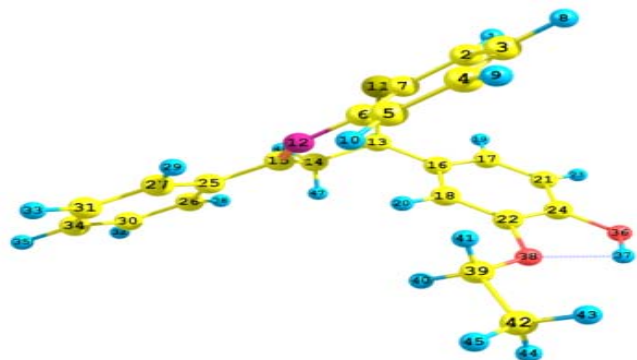
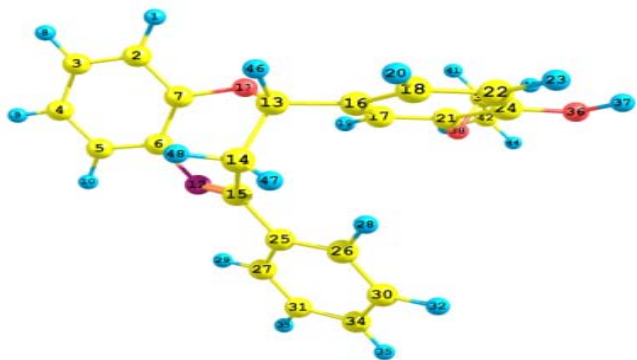
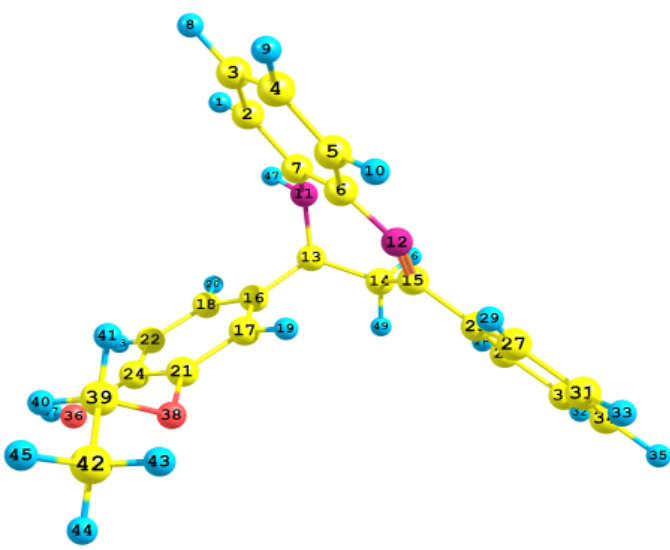
Inhibitor	Optimized structure	Inhibitor	Optimized structure
TMPBD		MDPBD	
EPBD		DPBD	
MBD		TMBD	

**Figure 8.2** HOMO and LUMO energy distribution for benzodiazepines

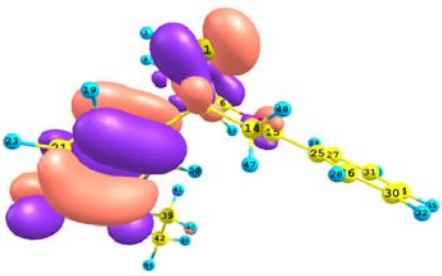
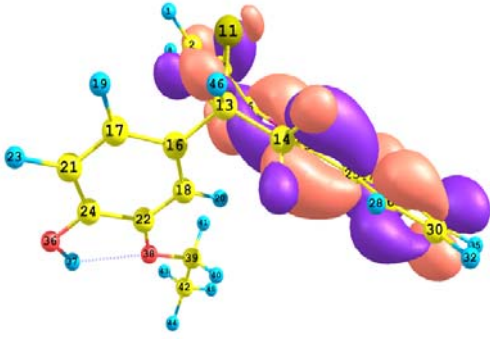
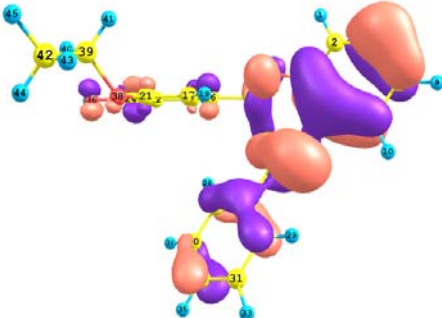
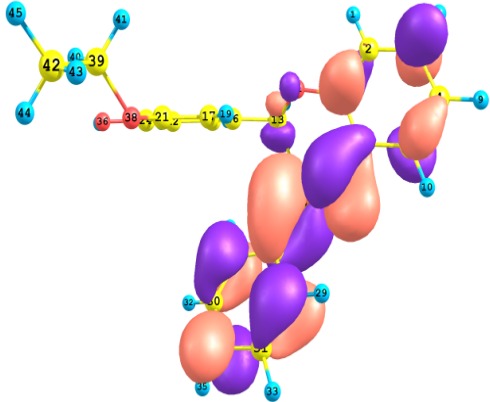
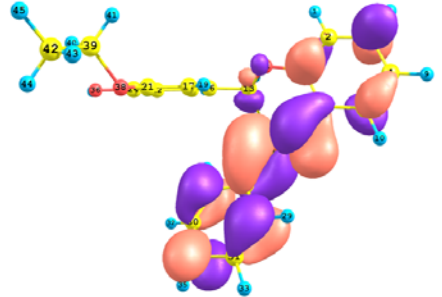
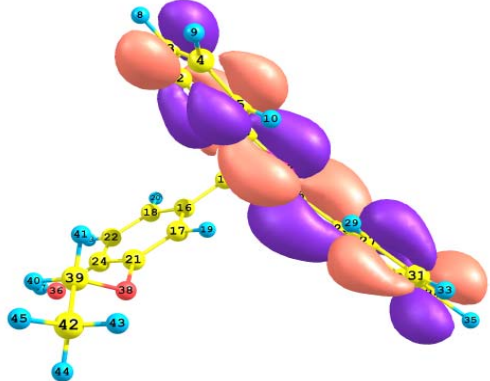


Inhibitor	HOMO	LUMO
MDPBD		
DPBD		
TMBD		

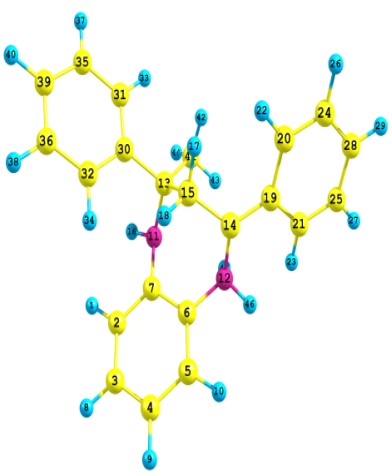
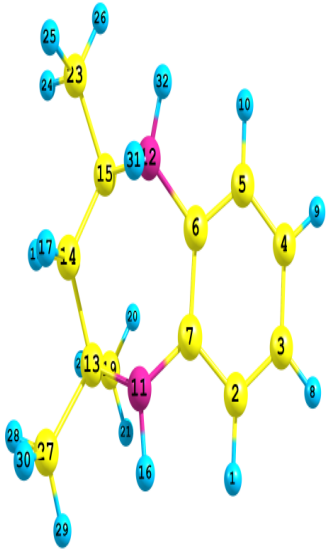
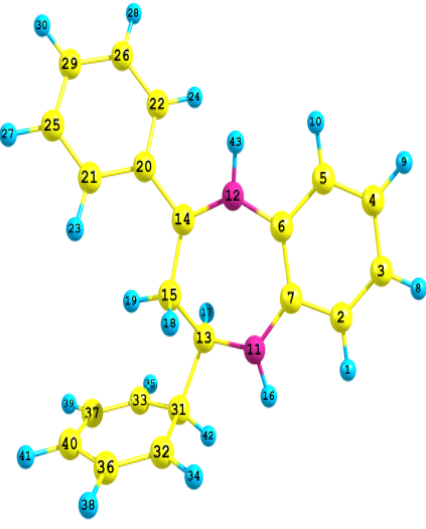
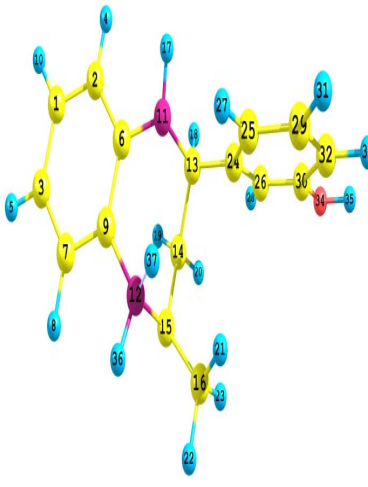
**Figure 8.3** Optimized geometry of benzodiazepines, benzothiazepines and benzoxazepines

Inhibitor	Optimized structure
<b>EPBTZ</b>	
<b>EPBOZ</b>	
<b>EPBD</b>	

**Figure 8.4** HOMO and LUMO energy distribution for benzodiazepines, benzothiazepines and benzoxazepines

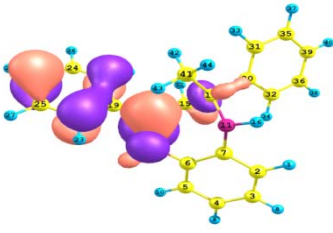
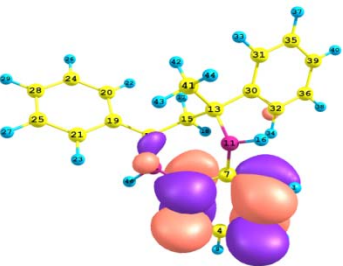
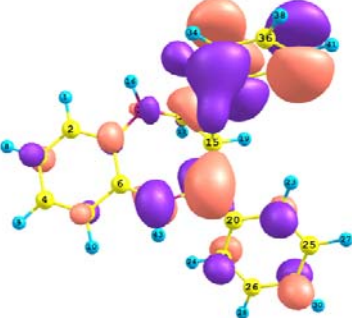
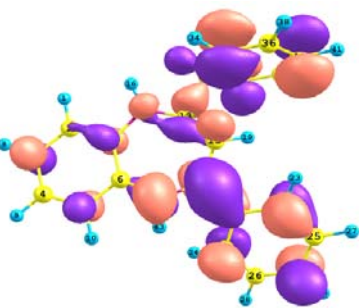
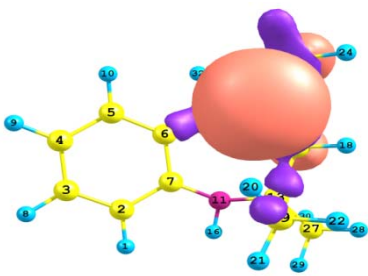
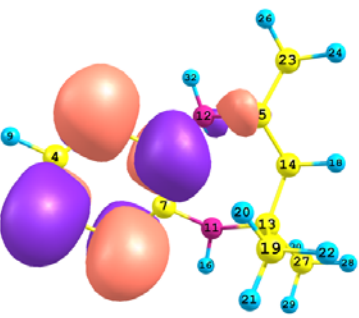
Inhibitor	HOMO	LUMO
EPBTZ	 <p>3D visualization of the Highest Occupied Molecular Orbital (HOMO) for EPBTZ. The molecule is shown with purple and red isosurfaces representing the orbital lobes. Atoms are numbered from 1 to 32.</p>	 <p>3D visualization of the Lowest Unoccupied Molecular Orbital (LUMO) for EPBTZ. The molecule is shown with purple and red isosurfaces representing the orbital lobes. Atoms are numbered from 1 to 42.</p>
EPBOZ	 <p>3D visualization of the Highest Occupied Molecular Orbital (HOMO) for EPBOZ. The molecule is shown with purple and red isosurfaces representing the orbital lobes. Atoms are numbered from 1 to 45.</p>	 <p>3D visualization of the Lowest Unoccupied Molecular Orbital (LUMO) for EPBOZ. The molecule is shown with purple and red isosurfaces representing the orbital lobes. Atoms are numbered from 1 to 45.</p>
EPBD	 <p>3D visualization of the Highest Occupied Molecular Orbital (HOMO) for EPBD. The molecule is shown with purple and red isosurfaces representing the orbital lobes. Atoms are numbered from 1 to 45.</p>	 <p>3D visualization of the Lowest Unoccupied Molecular Orbital (LUMO) for EPBD. The molecule is shown with purple and red isosurfaces representing the orbital lobes. Atoms are numbered from 1 to 45.</p>

**Figure 8.5** Optimized geometry for protonated benzodiazepines

Inhibitor	Optimized structure	Inhibitor	Optimized structure
<b>MDPBD</b>		<b>TMBD</b>	
<b>DPBD</b>		<b>MBD</b>	



**Figure 8.6** HOMO and LUMO energy distribution for protonated benzodiazepines

Inhibitor	HOMO	LUMO
MDPBD		
DPBD		
TMBD		
MBD	